IOPscience iopscience.iop.org

Home Search Collections Journals About Contact us My IOPscience

Quantum dynamics in quasiperiodic systems

This article has been downloaded from IOPscience. Please scroll down to see the full text article.

1995 J. Phys.: Condens. Matter 7 8383

(http://iopscience.iop.org/0953-8984/7/44/008)

View the table of contents for this issue, or go to the journal homepage for more

Download details:
IP Address: 171.66.16.151
The article was downloaded on 12/05/2010 at 22:23

Please note that terms and conditions apply.

J. Phys.: Condens. Matter 7 (1995) 8383–8404. Printed in the UK

Quantum dynamics in quasiperiodic systems

J X Zhong†‡ and R Mosseri†

† Groupe de Physique des Solides, Universités Paris 7 et Paris 6, Tour 23, 2 Place Jussieu, 75251 Paris Cédex 05, France

‡ Department of Physics, Xiangtan University, 411105 Hunan, People's Republic of China

Received 20 March 1995

Abstract. The electronic motion in quasiperiodic systems (the Harper model, the Fibonacci chain, two- and three-dimensional Fibonacci quasilattices) is studied, in the framework of a tight-binding Hamiltonian. The spreading with time of the wavepacket is described in terms of the behaviour of the autocorrelation function $C(t)$. It is found that, in all cases, $C(t) \sim t^{-\delta}$. For the Harper model with $\lambda < 2$, the motion of the electron is ballistic ($\delta = 1$), which goes against a previous estimate of $\delta = 0.84$. We show that this discrepancy is due to the neglect of a logarithmic contribution in the scaling analysis. For the Harper model with $\lambda = 2$ and the Fibonacci chain, the motion is non-ballistic with $0 < \delta < 1$. For the higher-dimensional Fibonacci quasilattices, $C(t)$ exhibits a transition from a ballistic to a non-ballistic behaviour, upon varying the modulation strength of the quasiperiodicity. The relation between $C(t)$ and the fractal dimensions of the spectral measure is also studied.

1. Introduction

In recent years, much attention has been paid to the investigation of the electronic properties of quasiperiodic systems, especially the energy spectrum and the wavefunctions. For 1D quasiperiodic structures, the spectral measure is singularly continuous and the eigenstates are critical, generally speaking [1–6]. For the high-dimensional quasiperiodic systems, the fact that it is difficult to get exact results in general (except for several special solvable quasilattices such as the high-dimensional Fibonacci quasilattices and the labyrinth tilings) implies that it is still hard to obtain a comprehensive understanding [3, 7–9]. Numerical calculations suggest that the spectrum of a high-dimensional quasilattice can be band-like with a finite number of gaps, fractal-like with zero band width, or a mixture with some parts band-like and some parts fractal-like. There is current interest [13–19] in the quantum dynamics of the systems which are associated with the complex spectra as stated above. The current work is directed at revealing the relationship between the electronic motion and the spectral measure. In addition, experimental results indicate that quasicrystals have unusual electronic transport properties [10]. Since conductivity is associated with the electronic motion in the system, it is important to study the dynamics of an electron in a quasiperiodic system. To study the dynamics, a direct approach is to investigate the time evolution of an electronic wavepacket. The procedure is as follows.

Consider a system with number of sites N. The Hamiltonian of the system has the following tight-binding form

$$H = \sum_i u_i |i\rangle\langle i| + \sum_{i,j} v_{ij} |i\rangle\langle j| \tag{1}$$

0953-8984/95/448383+22$19.50 © 1995 IOP Publishing Ltd

where u_i is the site energy at the ith site, v_{ij} are the hopping matrix elements. In our case, only nearest-neighbour interactions are considered. An electron is initially placed (at time $t = 0$) at a site position r_0 and is numbered $n = 0$ for the system. Then the time evolution of this state is given by the Schrödinger equation:

$$i\frac{d}{dt}\Psi(t) = H\Psi(t) \tag{2}$$

where $\Psi(t) = (\ldots, \psi_{n-1}, \psi_n, \psi_{n+1}, \ldots)^T$ is the wavefunction at time t, $\psi_n(t)$ is the coefficient of $\Psi(t)$ at the nth site. The initial condition is given by

$$|\psi_n(t = 0)| = \delta_{n,0}. \tag{3}$$

Equation (2) with the initial condition (3) can be solved by using, for instance, the finite time step Runge–Kutta method or by solving the static Schrödinger equation

$$H\Phi(E) = E\Phi(E) \tag{4}$$

where E is the eigenenergy and $\Phi(E)$ is the eigenvector, $\Phi(E) = (\ldots, \phi_{n-1}, \phi_n, \phi_{n+1}, \ldots)^T$. We use the latter approach. By solving (4), one gets all the eigenenergies E_j ($j = 1, 2, \ldots, N$) and the corresponding eigenstates $\Phi(E_j)$. Since $\Phi(E_j)$ is an orthonormal complete set, the wavefunction $\Psi(t)$ is then given by

$$\Psi(t) = \sum_j c_j \Phi(E_j) \exp(-iE_j t). \tag{5}$$

It follows from the initial condition (3) that

$$c_j = \phi_0^*(E_j). \tag{6}$$

Then the wavefunction $\Psi(t)$ is given by

$$\psi_n(t) = \sum_j \phi_0^*(E_j)\phi_n(E_j) \exp(-iE_j t) \tag{7}$$

where $\phi_0^*(E_j)$ is the complex conjugate of $\phi_0(E_j)$.

One can only treat finite size system numerically. In order to study long-time evolution one should take care that the wavepacket does not approach the boundaries. In our calculations, we use fixed boundary conditions.

Two quantities have been used to describe the motion of the electron. One is the mean square displacement $d(t)$ of the wavepacket defined as

$$d(t) = \sqrt{\langle(\Delta r)^2\rangle} = \sqrt{\sum_n |r_n - r_0|^2 \, |\psi(r_n, t)|^2} \tag{8}$$

The other is the autocorrelation function $P(t)$ (i.e. the probability of the wavepacket being in the initial position at time t)

$$P(t) = |\psi_0(t)|^2 \tag{9}$$

and its time-averaged version

$$C(t) = \frac{1}{t}\int_0^t P(t')\,dt'. \tag{10}$$

Numerical investigations of the motion of an electron in quasiperiodic systems were mainly done on typical models such as the Fibonacci chain and the Harper model.

The Harper model [1] is built on a 1D chain. The site energies of the Hamiltonian are $u_n = \lambda \cos(2\pi\sigma n)$, where $\sigma = (\sqrt{5} - 1)/2$ is the golden mean. The nearest-neighbour hopping integrals $v_{ij} = 1$ and all others are zero. The static version of this model has

been extensively studied and is known to display Anderson-like localization–delocalization transitions. When $\lambda < 2$, the spectrum is absolutely continuous and all the eigenstates are extended. In the region $\lambda > 2$, the spectrum is point-like and all the states are localized. $\lambda = 2$ is the critical point at which the spectrum is singularly continuous and the states are critical, i.e., neither localized nor extended.

The Fibonacci chain is the 1D paradigmatic model of quasicrystals [2–5]. The 'diagonal' model assumes that the hopping parameters $v_{ij} = 1$ and the site energies take two kinds of values, u_a and u_b, which forms a Fibonacci sequence. Without loss of generality, one can take $u_a = -u_b = -u$, $u > 0$. Then, the parameter u represents the strength of the quasiperiodic modulation. One can also introduce an 'off-diagonal' model by assuming that the site energies vanish ($u_i = 0$) and that the hopping parameters form a Fibonacci sequence taking two values 1 and v. It is known that the spectra of both models on the Fibonacci chain are singularly continuous.

The calculations of $d(t)$ for the Fibonacci chain and Harper models [13, 15, 18] show that the asymptotic behaviour of $d(t)$ follows a power-law growth

$$d(t) \sim t^{\beta}. \tag{11}$$

For the Harper model, the motion of the electron is ballistic with $\beta = 1$ for $\lambda < 2$ and $\beta = 0$ for $\lambda > 2$. For the Fibonacci chain model and the Harper model with $\lambda = 2$, one finds $0 < \beta < 1$. Guarneri [14] analytically proved that the power-law growth of $d(t)$ is a feature of 1D systems with singularly continuous measures. Moreover, an inequality relation between the exponent β and the spectral box-counting dimension D_1 is found:

$$\beta \geqslant D_1 \tag{12}$$

where D_1 is the information dimension of the spectral measure. Numerical results for the Harper model further confirm the above relation [18]. The calculation of $d(t)$ for 2D octagonal tiling was performed by Passaro *et al* [19]. It was found that $d(t)$ also exhibits a power-law growth with $0 < \beta < 1$.

The autocorrelation function has been used to study the electronic properties of various systems [11, 12, 16]. However, the relation between the decay of the autocorrelation function and the nature of the spectral measure of the system is still far from being understood. Numerical results [16] show that, for the Harper and Fibonacci chain models, $C(t)$ has a power-law decay

$$C(t) \sim t^{-\delta}. \tag{13}$$

For the Harper model, δ has been found to be $\delta = 0.84 \pm 0.01$; for $\lambda < 2$ for $\lambda > 2$, $\delta = 0$; for $\lambda = 2$, $C(t)$ has an anomalously low decay with exponent $\delta = 0.14 \pm 0.01$. For the Fibonacci chain diagonal model, δ decreases from 0.84 to 0 with the increase of the modulation strength. These numerical results are quite surprising since we know that the Fibonacci chain becomes a 1D periodic lattice if the modulation turns to zero we also know that the Harper model the spectrum is absolutely continuous for $\lambda < 2$. We are therefore led to ask the following questions:

(1) What is the difference in the behaviour of $C(t)$ in a periodic lattice, the Harper model with $\lambda < 2$ and the Fibonacci chain model in the limit of zero modulation?

(2) What is the origin of this special value 0.84?

(3) How does $C(t)$ decay with time in high-dimensional quasiperiodic systems?

To the best of our knowledge, almost all of the studies concerning the autocorrelation functions of quasiperiodic structures have focused on the 1D case. It is therefore very interesting to investigate the behaviour of $C(t)$ of high-dimensional quasiperiodic lattices and to look at the dimensionality dependence. Such a study is also important in order

to understand the transport properties of quasicrystals since the autocorrelation function describes the decay of the wavepacket, which is linked with the quantum diffusion of electrons.

This paper is organized as follows: in section 2, we study the autocorrelation functions of periodic systems in order to compare them with our results for other models. In section 3, the Harper model and 1D Fibonacci chain are considered. In section 4, we study the so-called 2D and 3D Fibonacci quasiperiodic lattices. The relationship between the autocorrelation function and the spectral measure is discussed in section 5. Discussions and conclusion are given in section 6.

2. The autocorrelation function of a periodic lattice

It is first necessary to understand the asymptotic behaviour of the autocorrelation function of a periodic lattice to further study quasiperiodic systems.

Let us study the usual 1D periodic chain, 2D square lattice and 3D cubic lattice. Let the distance between two first-neighbour sites be equal to a. The nearest-neighbour hopping parameters are $v_{ij} = v$ and the site energies are $u_i = u_0$. One can use Bloch theorem and analysis in the momentum space for the periodic lattice, because of the existence of periodic translational symmetry. In the 1D case, it is well known that the solution of (2) reads as

$$\psi_0(t) = \int \exp(-\mathrm{i}Et)\,\mathrm{d}\mu(E) = \frac{a}{2\pi}\int_{-\pi/a}^{\pi/a} \exp(-\mathrm{i}Et)\,\mathrm{d}k \tag{14}$$

with

$$E = u_0 + 2v\cos(ka) \qquad (-\pi \leqslant ka \leqslant \pi) \tag{15}$$

where k is the wavevector. It follows from (14) and (15) that

$$\text{1D} \qquad \psi_0(t) = \exp(-\mathrm{i}u_0t)J_0(2vt) \tag{16}$$

where $J_0(x)$ is the Bessel function of zero order. Similarly to the 1D case, it is easy to show that

$$\text{2D} \qquad \psi_0(t) = \exp(-\mathrm{i}u_0t)J_0^2(2vt) \tag{17}$$

$$\text{3D} \qquad \psi_0(t) = \exp(-\mathrm{i}u_0t)J_0^3(2vt). \tag{18}$$

The autocorrelation functions $P(t)$ and $C(t)$ are then given by

$$P(t) = J_0^{2D}(2vt) \tag{19}$$

$$C(t) = \frac{1}{t}\int_0^t J_0^{2D}(2vt')\,\mathrm{d}t' \tag{20}$$

where D is the dimension of the periodic lattices. Without loss of generality, we assume $u_0 = 0$ and $v = 1$ in the following analysis.

For the Bessel function $J_0(x)$, one has the following asymptotic behaviour

$$J_0(x) \sim \sqrt{\frac{2}{\pi x}}\cos(x - \pi/4) \qquad (x \to \infty) \tag{21}$$

which leads to

$$P(t) \sim t^{-D}. \tag{22}$$

Since

$$J_0^{2D}(x) \leqslant \frac{2}{\pi}x^{-D} \qquad (x \to \infty) \tag{23}$$

the integral

$$I_D = \int_0^\infty J_0^{2D}(x)\,\mathrm{d}x \tag{24}$$

is then convergent for $D = 2$ and $D = 3$. We rewrite (20) as

$$C(t) = \frac{1}{2t}\left[\int_0^\infty J_0^{2D}(x)\,\mathrm{d}x - \int_{2t}^\infty J_0^{2D}(x)\,\mathrm{d}x\right]. \tag{25}$$

From (21), (24) and (25), we have

$$\text{2D} \qquad C(t) \sim t^{-1}\left[\frac{1}{2}I_2 - \frac{3}{8\pi^2}t^{-1} + \mathrm{O}(t^{-2})\right] \tag{26}$$

$$\text{3D} \qquad C(t) \sim t^{-1}\left[\frac{1}{2}I_3 - \frac{5}{32\pi^3}t^{-2} + \mathrm{O}(t^{-3})\right]. \tag{27}$$

To analyse the 1D case, let us take a time such that t_0 is large. If $t > t_0$, the asymptotic behaviour (21) can be used. We then rewrite $C(t)$ as

$$C(t) = A(t) + B(t) \tag{28}$$

$$A(t) = \frac{1}{2t}\int_0^{2t_0} J_0^2(x)\,\mathrm{d}x \tag{29}$$

$$B(t) = \frac{1}{2t}\int_{2t_0}^{2t} J_0^2(x)\,\mathrm{d}x \tag{30}$$

since $|J_0(x)| \leqslant 1$, then

$$A(t) \leqslant \frac{t_0}{t}. \tag{31}$$

Taking the limit $t \to \infty$ and using (21), we find

$$B(t) \sim \frac{1}{2\pi t}(\ln t - \ln t_0) + \frac{1}{2\pi t}\int_{2t_0}^{2t} \frac{\sin 2x}{x}\,\mathrm{d}x \tag{32}$$

and since the integral

$$\int_{2t_0}^{2t} \frac{\sin 2x}{x}\,\mathrm{d}x \tag{33}$$

is convergent, we finally have

$$C(t) \sim \frac{1}{2\pi}t^{-1}\ln t. \tag{34}$$

We have calculated numerically the integration $tC(t)$, by either directly diagonalizing the Hamiltonian matrix and using (7) or by using the Bessel function (see figure 1). We find that the results agree with the analytical conclusion,

$$\text{1D}: \qquad C(t) \sim (c_0 + c_1 \log t)t^{-1} \tag{35}$$

with $c_0 = 0.529 \pm 0.001$ and $c_1 = 0.366 \pm 0.001$. We would like to stress that, due to the presence of the logarithmic contribution, it is rather difficult to extract a meaningful exponent if one performs, for instance, a least-squares fit directly to the curve of $\log C(t)$ versus $\log t$ in a finite time scale. For example, in the case of the 1D periodic chain, one can express $C(t)$ as $C(t) \sim t^{-\delta}$ with

$$\delta = 1 - \frac{\log[c_0 + c_1 \log t]}{\log t}. \tag{36}$$

Obviously δ varies with time and approaches 1 asymptotically. If $t < 10^3$, we find $\delta \approx 0.84$. Since, from a numerical point of view, one can use clusters of limited size, the time scale chosen is then also limited, and one should therefore be very careful in the scaling analysis.

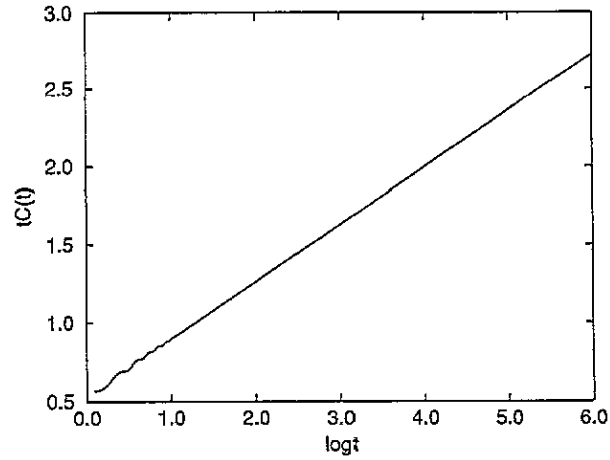

Figure 1. Plot of $tC(t)$ versus $\log t$ for the 1D periodic lattice.

3. 1D quasiperiodic systems

On the basis of the above results for periodic lattices, we now study the decay of $C(t)$ for 1D quasiperiodic systems. The numerical calculations are performed along the lines of those introduced in section 1. Two typical quasiperiodic Hamiltonian models, the Harper model and the Fibonacci model are investigated here.

3.1. The Harper model

The system studied has $N \approx 3000$ sites. The electron is initially placed at the zeroth site. The decay of $C(t)$ is presented in figure 2. Our numerical calculation indicates that, for $\lambda > 2$, $C(t) \sim t^0$. In the case of $\lambda = 2$, $C(t) \sim f(\log t)t^{-\delta}$, where $\delta = 0.13 \pm 0.01$ and $f(x)$ is a periodic function with period 0.49 ± 0.01. The exponents for these two cases are in agreement with previous calculations [16]. However, $C(t)$ for $\lambda = 2$ given in [16] does not show periodic oscillation. Since the spectrum for $\lambda = 2$ is fractal-like, one expects that $C(t)$ will oscillate with time since $C(t)$ is the Fourier–Stieltjes transform of the spectral measure. We shall discuss this later. For $\lambda < 2$, Ketzmerick *et al* [16] found that $C(t) \sim t^{-\delta}$ with $\delta = 0.84 \pm 0.01$. In our calculation, we also find this value if we do a standard least-squares fit to $\log C(t)$ versus $\log t$. However, if we choose a different time scale to do the fit, we find that the exponent varies with the chosen time scale. According to what we have learnt in the 1D periodic lattice, we plot $tC(t)$ versus $\log t$ in figure 2(b). We find that, similar to the 1D periodic lattice, $C(t) \sim (c_0 + c_1 \log t)t^{-1}$ for $\lambda < 2$, with $c_0 = 0.30 \pm 0.01$ and $c_1 = 1.65 \pm 0.01$. As stated above, for $\lambda < 2$, the spectrum is absolutely continuous and the states are extended. Our result shows that, in this case, the asymptotic decay of $C(t)$ has the same form as for the 1D periodic lattice.

3.2. The Fibonacci chain method

We now study the diagonal and off-diagonal models. The behaviour of $C(t)$ for various modulations is illustrated in figures 3 and 4, for the diagonal and off-diagonal models, respectively.

Firstly, we would like to point out that, in the case $u = 0$ or $v = 1$, which corresponds to

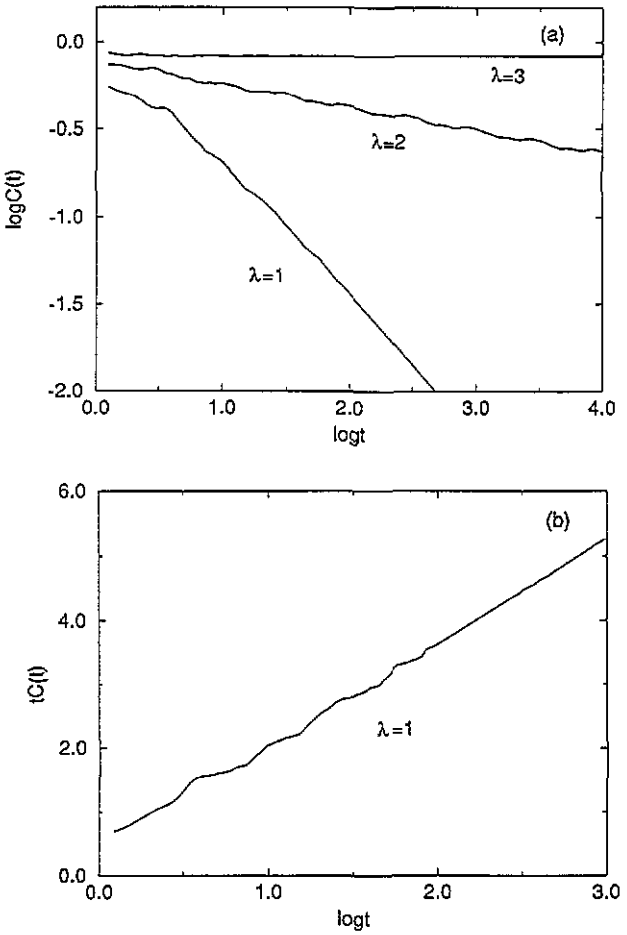

Figure 2. Autocorrelation function for the Harper model; (a) $\log C(t)$ versus $\log t$ for $\lambda = 1, 2, 3$; (b) $tC(t)$ versus $\log t$ for $\lambda = 1$.

the periodic case, our numerical results show that $C(t)$ is the same as that which we obtain by taking the integration of the Bessel function as explained in section 2. This indicates that, in the periodic limit $u = 0$ or $v = 1$ of the Fibonacci chain model, $C(t) \sim t^{-\delta}$ with $\lim_{t\to\infty} \delta = 1$, and not 0.84 as obtained by Ketzmerick *et al* [16]. Furthermore, we find that the curve $\log C(t)$ versus $\log t$ presented in figures 3 and 4 cannot be well fitted by the least-squares fit in the region of weak modulations. Instead, $C(t)$ can be fitted in general as

$$tC(t) \sim c_0 + c_1 t^{\gamma} \qquad 0 < \gamma < 1. \tag{37}$$

For instance, for the diagonal model with $u = 0.05$, $c_0 = -1.341 \pm 0.001$, $c_1 = 1.912 \pm 0.001$ and $\gamma = 0.07 \pm 0.01$; if $u = 0.1$, then $c_0 = -0.286 \pm 0.001$, $c_1 = 0.866 \pm 0.001$ and $\gamma = 0.14 \pm 0.01$. The exponent γ increases with an increase in the modulation strength. This property can be clearly seen in figure 5. The relation (37) indicates that $C(t)$ goes to zero asymptotically following the power law $C(t) \sim t^{-\delta}$, where $\delta = 1 - \gamma$ and $0 < \delta < 1$. It is found that when $u > 0.2$ or $v > 1.2$, δ can be well evaluated by doing the least-squares fit directly to the curve of $\log C(t)$ versus $\log t$. This is because for large u or v, γ is large and the second term in (37) then plays the dominant rule even for small time scales.

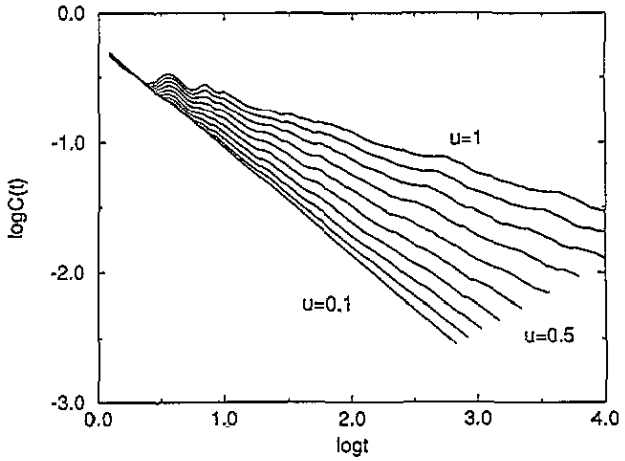

Figure 3. Log–log plot of $C(t)$ versus t for the Fibonacci chain (diagonal model) with $u = 0.1$, 0.2, 0.3, ..., 0.9 and 1, sucessively.

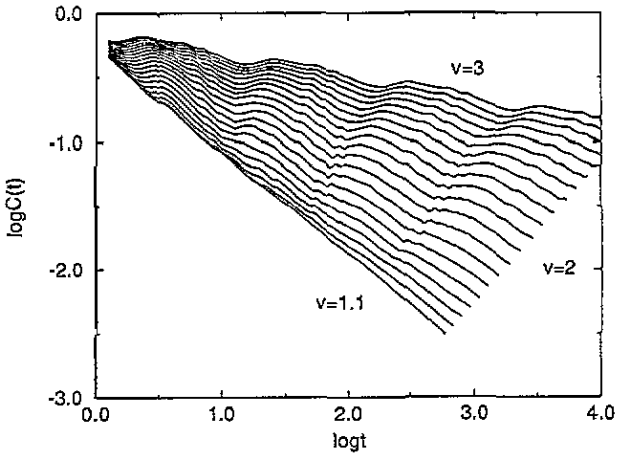

Figure 4. Log–log plot of $C(t)$ versus t for the Fibonacci chain (off-diagonal model) with $v =$ 1.1, 1.2, 1.3, ..., 2.9 and 3, sucessively.

The reason why the previous calculation gives $\delta < 0.84$ is the following. In the region of weak modulation, γ is small. If the time scale is not large enough, c_0 can play a role. In fact, we also find the value 0.84 when we do the least-squares fit directly to the curve of $\log C(t)$ versus $\log t$ in the limit $u \to 0$ or $v \to 1$. The dependence of the exponent δ on the modulation strength is illustrated in figures 10 and 11.

4. The 2D and 3D Fibonacci quasilattices

Several solvable high-dimensional quasilattices generated from 1D quasiperiodic models have been proposed to understand the spectral properties of high-dimensional quasicrystals [7–9]. Among these, the 2D Fibonacci quasilattices have been studied in detail [8, 9]. Recently, the 3D Fibonacci quasilattice has been used by C Sire [3] to analyse the electronic

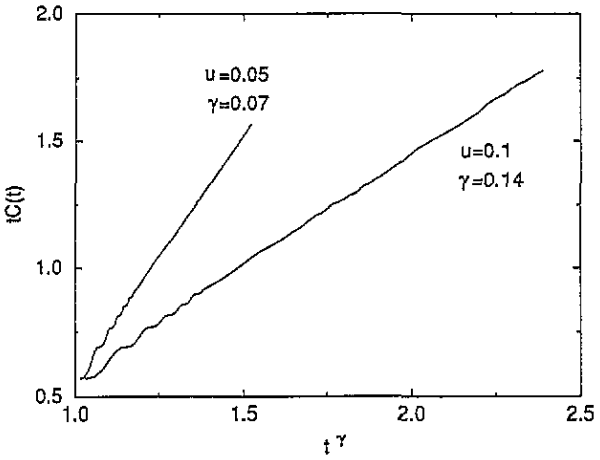

Figure 5. Plot of $tC(t)$ versus t^{γ} for the Fibonacci chain (diagonal model) with $u = 0.05$ and $u = 0.1$.

transport properties of real quasicrystals by calculating the Boltzmann conductivity. 2D (3D) Fibonacci quasilattices are built on square (cubic) lattices with a tight-binding Hamiltonian related to the 1D Fibonacci model.

(i) Diagonal model. The nearest-neighbour hopping integrals are $v_{ij} = 1$; the site energy u_i at the ith site is separable, i.e., $u_i = u_{ix} + u_{iy}$ (or $u_i = u_{ix} + u_{iy} + u_{iz}$ for the 3D case), where $u_{ik}(k = x, y, z)$ independently forms the Fibonacci sequence with two kinds of values $-u$ and u.

(ii) Off-diagonal model. The site energies are $u_i = 0$. The hopping parameters along the x and y axes for 2D or x, y and z for 3D follow the Fibonacci sequence, with two kinds of parameters 1 and v.

It has been found that the spectral properties of the above models depend on the parameters of the Hamiltonian [8,9]. The spectrum can be band-like with finite number of gaps, fractal-like with zero band width or a mixture of both with some parts band-like and some parts fractal-like. For the 2D diagonal model two kinds of transition exist about the nature of the measure [9]. In the region $0 < u < 0.6$, the spectrum is band-like with finite a number of gaps. For $0.6 < u < 2.0$, the spectrum contains fractal parts while the total band width is still finite. If $u > 2.0$, the measure is then fractal-like with zero band width. An interesting question is therefore: do these transitions of the spectra correspond to transitions of the electronic dynamics in the system?

Let us use ϕ_{mn} and ϕ_{mnp} to denote the wavefunction at the site numbered by (m, n) and (m, n, p), for 2D and 3D quasilattices, respectively. One can show [8,9] that the eigenenergies and the eigenstates of 2D and 3D Fibonacci quasilattices can be given by

$$E = E_x + E_y \tag{38}$$

$$\phi_{mn}(E) = \phi_m(E_x)\phi_n(E_y) \tag{39}$$

and

$$E = E_x + E_y + E_z \tag{40}$$

$$\phi_{mnp}(E) = \phi_m(E_x)\phi_n(E_y)\phi_p(E_z) \tag{41}$$

respectively, where E_x, E_y and E_z are the eigenenergies of the 1D Fibonacci chain, and $\phi_m(E_x)$, $\phi_n(E_y)$ and $\phi_p(E_z)$ are the corresponding eigenstates.

We now study the autocorrelation functions of 2D and 3D Fibonacci quasilattices for the diagonal and off-diagonal models. In the following, we prove that the autocorrelation function $C(t)$ of these 2D and 3D Fibonacci quasilattices can be calculated from knowledge of the corresponding quantity in the 1D Fibonacci chain. We shall focus on the 2D Fibonacci quasilattice. The treatment of the 3D case follows the same procedure.

By solving the static Schrödinger equation of the 1D Fibonacci chain with N sites, we obtain N eigenenergies $E_j (j = 1, 2, 3, \ldots N)$ and the corresponding eigenstates $\phi_m(E_j)$. Since the eigenstates of 1D Fibonacci chain form a complete orthonomal set, one has

$$\sum_m \phi_m^*(E_i)\phi_m(E_j) = \delta_{ij} \tag{42}$$

$$\sum_{E_j} \phi_m^*(E_j)\phi_n(E_j) = \delta_{mn}. \tag{43}$$

Using (38), (39), (42) and (43), we have

$$\sum_{mn} \phi_{mn}^*(E)\phi_{mn}(E') = \delta(E - E') \tag{44}$$

$$\sum_E \phi_{mn}^*(E)\phi_{m'n'}(E) = \delta_{mm'}\delta_{nn'} \tag{45}$$

where E is the eigenenergy of the 2D system. (44) and (45) indicate that the $N \times N$ eigenstates obtained by the products of the eigenstates of the 1D Fibonacci chain are still complete and orthonomal. Now, suppose that an electron is initially placed at the site numbered $(m_0 n_0)$. According to (7), the wavefunction at site mn at time t is given by

$$\psi_{mn}(t) = \sum_E \exp(-\mathrm{i}Et)\phi_{m_0 n_0}^*(E)\phi_{mn}(E). \tag{46}$$

Using (38) and (39), we have

$$\psi_{mn}(t) = \psi_m(t)\psi_n(t) \tag{47}$$

where $\psi_m(t)$ and $\psi_n(t)$ are given by the 1D chain

$$\psi_m(t) = \sum_{E_x} \exp(-\mathrm{i}E_x t)\phi_{m_0}^*(E_x)\phi_m(E_x) \tag{48}$$

$$\psi_n(t) = \sum_{E_y} \exp(-\mathrm{i}E_y t)\phi_{n_0}^*(E_y)\phi_n(E_y). \tag{49}$$

(47) gives the autocorrelation functions $P(t)$ and $C(t)$ of the 2D Fibonacci quasilattice

$$P(t) = P_{m_0}(t)P_{n_0}(t) \tag{50}$$

$$C(t) = \frac{1}{t}\int_0^t P_{m_0}(t')P_{n_0}(t')\,\mathrm{d}t' \tag{51}$$

where $P_{m_0}(t)$ and $P_{n_0}(t)$ are the probabilities of the 1D Fibonacci chain. For the 3D Fibonacci quasilattice, if the electron is initially placed at the site numbered as $m_0 n_0 p_0$, the same analysis gives

$$P(t) = P_{m_0}(t)P_{n_0}(t)P_{p_0}(t) \tag{52}$$

$$C(t) = \frac{1}{t}\int_0^t P_{m_0}(t')P_{n_0}(t')P_{p_0}(t')\,\mathrm{d}t'. \tag{53}$$

From (50)–(53), one sees that the autocorrelation functions of 2D and 3D Fibonacci quasilattices can be calculated from the corresponding quanties in the 1D Fibonacci chain.

As a consequence, we can treat large enough high-dimensional systems to get information about the long-time behaviour of the autocorrelation functions. In our calculation, the size of the Fibonacci chain is $N \approx 3000$. The 2D and 3D quasilattices studied therefore have $N \approx 10^7$ and 10^{10} sites, respectively.

We numerically calculate $C(t)$ for 2D and 3D Fibonacci quasilattices by using the function $P(t)$ previously derived for the Fibonacci chain

$$C(t) = \frac{1}{t}\int_0^t P^D(t')\,dt' \tag{54}$$

where D is the dimension. This corresponds to the case $m_0 = n_0$ for 2D and $m_0 = n_0 = p_0$ for 3D. As an example, the decay of $C(t)$ with various Hamiltonian parameters are presented in figures 6 and 7 for the off-diagonal model. At first sight, figures 6 and 7 show the power-law decay $C(t) \sim t^{-\delta}$. According to the scaling analysis of 1D quasiperiodic systems, and especially after having stressed the role of the subdominant parts occurring in the periodic lattices in (26) and (27), a careful treatment is still very necessary in order to get the exponent δ.

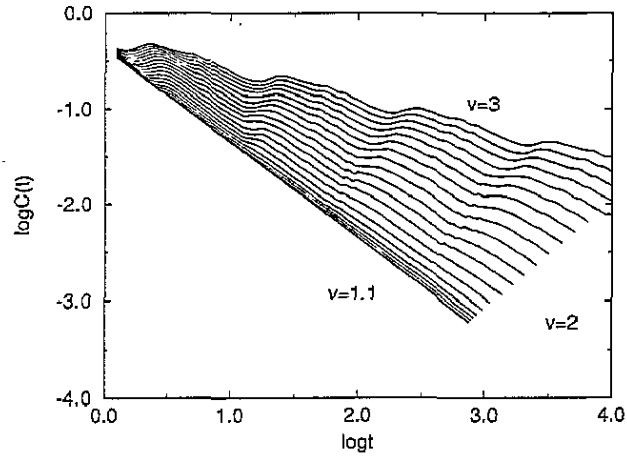

Figure 6. Log–log plot of $C(t)$ versus t for the 2D Fibonacci quasilattice (off-diagonal model) with various modulations (as in figure 4).

We have seen that, for the Fibonacci chain, $C(t) \sim t^{-\delta}$ with $0 < \delta < 1$. Here, the numerical results show that, unlike the 1D case, there exist two different ranges of parameters which correspond to different decays of $C(t)$ for the high-dimensional quasilattices. In region I, $\delta = 1$, irrespective of the modulation strength of the quasiperiodicity. In region II, $0 < \delta < 1$ and δ decreases as the modulation strength increases. Let us analyse the 2D and 3D Fibonacci diagonal models in more detail. We find that $C(t)$ in these two regions shows the following behaviour.

Region I $\quad 0 \leqslant u < u_c \qquad C(t) \sim (c_0 - c_1 t^{-\gamma})t^{-1} \qquad 0 < \gamma \leqslant D - 1 \tag{55}$

where $u_c \approx 0.6$ when $D = 2$ and $u_c \approx 0.9$ when $D = 3$, respectively. This behaviour is clearly seen in figures 8 and 9. The exponent γ decreases from $D - 1$ to 0 as u increases. For $u = 0$, we find $\gamma = 1$ ($\gamma = 2$) for the 2D (3D) periodic lattice, as expected. Formula (55) gives $\lim t \to \infty$, $C(t) \sim t^{-1}$.

Region II $\quad u > u_c \qquad C(t) \sim (c_0 + c_1 t^{\gamma})t^{-1} \qquad 0 < \gamma < 1 \tag{56}$

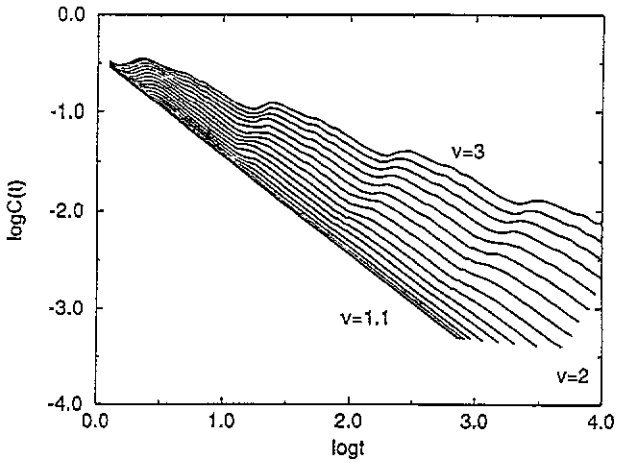

Figure 7. Log–log plot of $C(t)$ versus t for the 3D Fibonacci quasilattice (off-diagonal model) with the same parameters as in figure 4.

In this region, $C(t)$ exhibits the same behaviour as for the Fibonacci chain model. We illustrate this behaviour in figure 9. The exponent γ increases as u increases. So for large u, the exponent δ can be evaluated by fitting the curve $\log C(t)$ versus $\log t$. It follows from (56) that $C(t) \sim t^{-\delta}$ with $0 < \delta < 1$ for $u > u_c$. For the 2D and 3D off-diagonal models, the decay of $C(t)$ displays the same properties. We find that the critical values v_c corresponding to the crossover of $C(t)$ are $v_c \approx 1.7$ and $v_c \approx 2.1$ for 2D and 3D quasilattices, respectively. In figures 10 and 11, we plot the dependence of the exponent δ on the modulations u and v.

So in conclusion, we have shown that the autocorrelation functions $C(t)$ of 1D, 2D and 3D Fibonacci quasilattices display a power-law decay $C(t) \sim t^{-\delta}$. For a 1D Fibonacci chain, we have $0 < \delta < 1$, which corresponds to a non-ballistic diffusion of the electron. In contrast to the 1D case, we find a crossover for 2D and 3D Fibonacci quasilattices, i.e., from ballistic-like behaviour to a non-ballistic-like behaviour. If the modulation strength is less than a critical value, $C(t)$ still has the form $C(t) \sim t^{-1}$ characteristic of a ballistic motion of the electron in periodic lattices. If the modulation is larger than this critical value, $C(t)$ then behaves as $C(t) \sim t^{-\delta}$ with $0 < \delta < 1$.

The crossover of the exponent δ in higher-dimensional Fibonacci quasilattices can be understood using the following argument. (Note: this argument has been proposed by C Sire and J Bellissard. The authors are very grateful to them.) For the 1D Fibonacci chain, we have $C(t) \sim t^{-\delta_1}$ with $0 < \delta_1 < 1$. Then one has

$$P(t) \sim t^{-\delta_1} \qquad 0 < \delta_1 < 1. \tag{57}$$

According to (50) and (52), one can see that the probability $P(t)$ for 2D and 3D Fibonacci quasilattices behaves asymptotically as $P(t) \sim t^{-\alpha}$ where $0 < \alpha < 2$ for a 2D Fibonacci quasilattice and $0 < \alpha < 3$ for 3D Fibonacci quasilattice, respectively. We know that, if $P(t) \sim t^{-\alpha}$ and $\alpha > 1$, the integral $tC(t) = \int_0^t P(t')\,dt'$ is convergent (note that $P(t = 0) = 1$). Thus one has $C(t) \sim t^{-1}$. Since δ_1 continuously decreases from 1 to 0, one concludes that there exists a region in which the integral $tC(t)$ is convergent and $C(t) \sim t^{-1}$. Now let us look again at our numerical results. It follows from (54) and the above discussions that

$$D\delta_1 > 1 \implies C(t) \sim t^{-1} \qquad D\delta_1 < 1 \implies C(t) \sim t^{-D\delta_1} \tag{58}$$

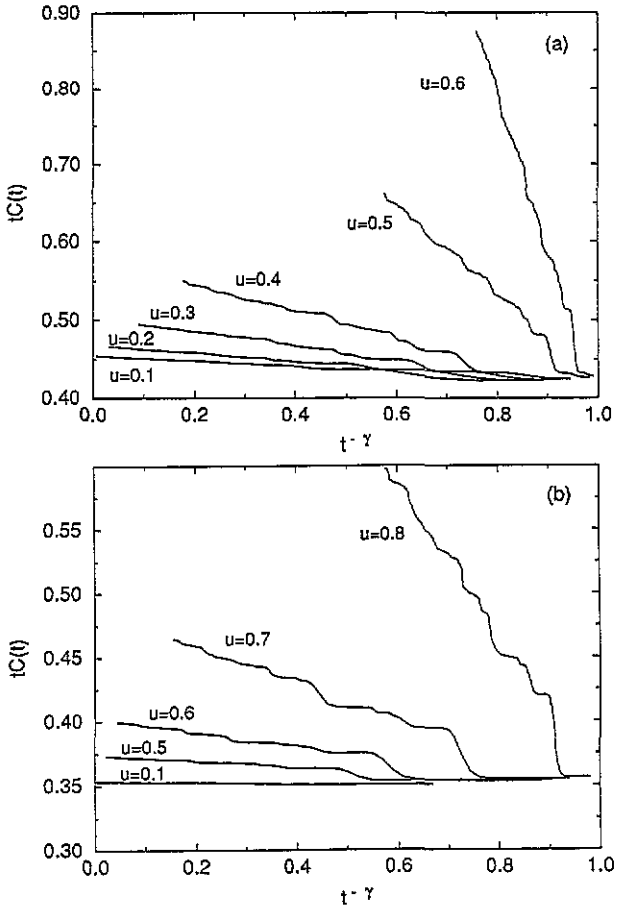

Figure 8. Plot of $tC(t)$ versus $t^{-\gamma}$ for the 2D and 3D Fibonacci quasilattices (diagonal model): (a) 2D Fibonacci quasilattice with $u = 0.1, 0.2, 0.3, 0.4, 0.5, 0.6$ corresponding to $\gamma = 0.7, 0.5, 0.35, 0.25, 0.08, 0.04$, respectively; (b) 3D Fibonacci quasilattice with $u = 0.1, 0.5, 0.6, 0.7, 0.8$ corresponding to $\gamma = 1.8, 0.55, 0.45, 0.27, 0.08$, respectively.

where δ_1 is the scaling exponent of $C(t)$ for a 1D Fibonacci chain. Therefore $D\delta_1 = 1$ gives the critical point of the crossover which corresponds to the modulation strength where the exponent δ_1 of the 1D Fibonacci chain has the value $\delta_1 = \frac{1}{2}$ and $\delta_1 = \frac{1}{3}$ for 2D and 3D Fibonacci quasilattices, respectively. For the diagonal model, the u_c given by the above argument are $u_c \approx 0.6$ and $u_c \approx 0.9$ for 2D and 3D systems (see figure 10), which agrees quite well with the numerical results. Moreover, we find that the exponent δ is D times that of the 1D case. The above argument is also in good agreement with the numerical results of the off-diagonal models.

5. The autocorrelation function and the spectral measure

The autocorrelation function is directly related to the spectral measure of the system. The probability $P(t)$ can be written as

$$P(t) = \left| \int \exp(-iEt)\, d\mu(E) \right|^2 \tag{59}$$

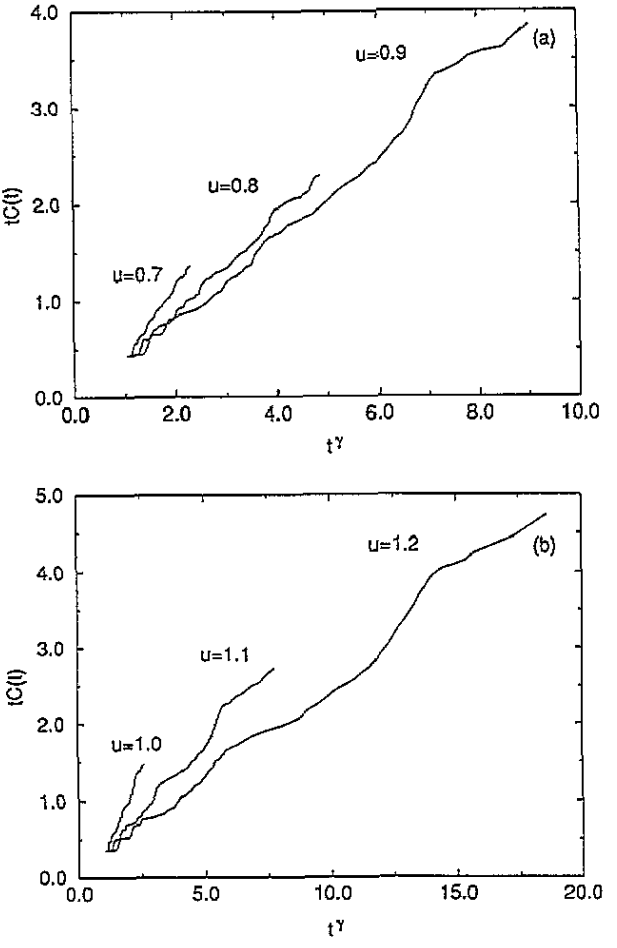

Figure 9. Plot of $tC(t)$ versus t^γ for the 2D and 3D Fibonacci quasilattices (diagonal model); (a) 2D Fibonacci quasilattice with $u = 0.7, 0.8, 0.9$ corresponding to $\gamma = 0.12, 0.23, 0.32$, respectively; (b) 3D Fibonacci quasilattice with $u = 1.0, 1.1, 1.2$ corresponding to $\gamma = 0.13, 0.27, 0.4$, respectively.

which is the square of the modulus of the Fourier–Stieltjes transform of the measure $\mu(E)$ at the site where the electron is initially placed. It has been shown [16] that the power-law decay of $C(t)$ is related to the fractal dimension D_2 of the spectral measures of singularly continuous or absolutely continuous spectra. The argument is as follows.

The fractal dimension D_2 (the correlation dimension of the measure) is defined as

$$R(l) = \int \mathrm{d}\mu(E) \int_{E-l/2}^{E+l/2} \mathrm{d}\mu(E') \sim l^{D_2} \qquad (l \to 0) \tag{60}$$

where $R(l)$ is the spectral probability. Using the box function

$$\chi_A(E, E') = \begin{cases} 1 & E' \in A \\ 0 & E' \notin A \end{cases} \tag{61}$$

with $A = [E - l/2, E + l/2]$, $R(l)$ can be rewritten as

$$R(l) = \int \mathrm{d}\mu(E) \int \chi_A(E, E')\, \mathrm{d}\mu(E'). \tag{62}$$

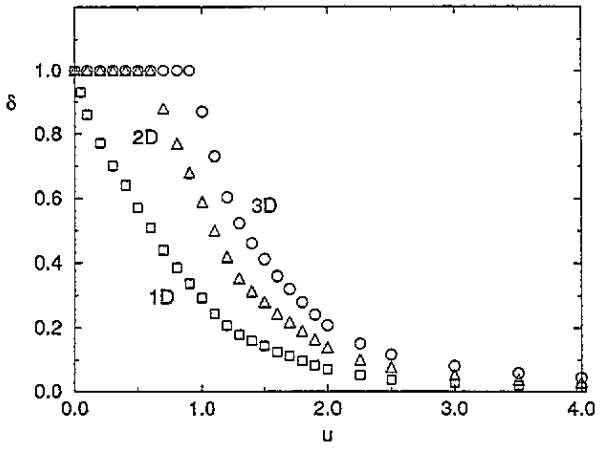

Figure 10. Exponent δ versus the modulation strength u for $C(t)(\sim t^{-\delta})$ in the 1D, 2D and 3D Fibonacci quasilattices (diagonal model).

The Fourier transform of the above box function reads

$$\chi_A(E, E') = \frac{1}{\pi}\int_{-\infty}^{+\infty} \exp\left[\mathrm{i}(E - E')\tau\right]\frac{\sin(l\tau/2)}{\tau}\,\mathrm{d}\tau. \tag{63}$$

Inserting (63) into (62), one has

$$R(l) = \frac{1}{\pi}\int \mathrm{d}\mu(E)\int\left\{\int_{-\infty}^{+\infty} \exp\left[\mathrm{i}(E - E')\tau\right]\frac{\sin(l\tau/2)}{\tau}\,\mathrm{d}\tau\right\}\mathrm{d}\mu(E'). \tag{64}$$

According to the properties of the Fourier–Stieltjes transform, for a singularly continuous or absolutely continuous measure $\mu(E)$, if the measure is of bounded variation (this is the usual case for a tight-binding Hamiltonian problem)

$$R(l) = \frac{1}{\pi}\int_{-\infty}^{+\infty}\frac{\sin(l\tau/2)}{\tau}\,\mathrm{d}\tau\int \exp(\mathrm{i}E\tau)\,\mathrm{d}\mu(E)\int \exp(-\mathrm{i}E'\tau)\,\mathrm{d}\mu(E'). \tag{65}$$

Finally one has

$$R(l) = \frac{2}{\pi}\int_{-\infty}^{+\infty} P(\tau)\frac{\sin(l\tau/2)}{\tau}\,\mathrm{d}\tau. \tag{66}$$

Assuming a pure power-law behaviour either for $R(l)$ or for $C(t)$, Ketzmerick *et al* [16] have claimed that they can prove

$$R(l) \sim l^{\delta}\ (l \to 0) \iff C(t) \sim t^{-\delta}\ (t \to \infty) \tag{67}$$

for $0 < \delta < 1$ and $\delta = D_2$ according to (60). However the proof is not given. Using a technique similar to that developed in the scaling analysis of Green's function [6], we present a proof for the above relationship between the scaling behaviours of $R(l)$ and $C(t)$.

Before discussing the relation between $R(l)$ and $C(t)$, we need to give a clear definition of the scaling exponent δ. For a positive function $g(\epsilon)$ in [0,1], we consider the following integral

$$J_g(\delta') = \int_0^1 \frac{g(\epsilon)}{\epsilon^{1+\delta'}}\,\mathrm{d}\epsilon \tag{68}$$

We shall say that $g(\epsilon) \sim \epsilon^{\delta}$, if $J_g(\delta')$ converges for $\delta' < \delta$ and diverges if $\delta' > \delta$. For $\delta_1' \leqslant \delta_2'$, we have $J_g(\delta_1') \leqslant J_g(\delta_2')$. Then if $g(\epsilon) \sim \epsilon^{\delta}$, the scaling exponent δ can be defined by

$$\delta = \mathrm{Sup}\{\delta', J_g(\delta') < +\infty\}. \tag{69}$$

From (66), we have

$$R(l) = \frac{2}{\pi} \int_0^{+\infty} P\left(\frac{2x}{l}\right) \frac{\sin x}{x} \, \mathrm{d}x. \tag{70}$$

Now we consider the following integral

$$J_R(\delta') = \int_0^1 \frac{R(l)}{l^{\delta'+1}} \, \mathrm{d}l. \tag{71}$$

Use (70) and let $2x/l = \xi$,

$$\begin{aligned} J_R(\delta') &= \frac{2}{\pi} \int_x^{+\infty} P(\xi) \xi^{\delta'-1} \, \mathrm{d}\xi \int_0^{+\infty} \frac{\sin(x/2)}{x^{\delta'+1}} \, \mathrm{d}x \\ &= \frac{2}{\pi} \int_0^{+\infty} P(\xi) \xi^{\delta'-1} \, \mathrm{d}\xi \int_0^{\xi} \frac{\sin(x/2)}{x^{\delta'+1}} \, \mathrm{d}x. \end{aligned} \tag{72}$$

Let $Q(t) = tC(t)$, then we have

$$J_R(\delta') = \frac{2}{\pi} \int_0^{+\infty} \xi^{\delta'-1} \, \mathrm{d}Q(\xi) \int_0^{\xi} \frac{\sin(x/2)}{x^{\delta'+1}} \, \mathrm{d}x. \tag{73}$$

Inspecting the integral we have

$$J_R'(\delta') = \int_0^{+\infty} \xi^{\delta'-1} \, \mathrm{d}Q(\xi) \tag{74}$$

since

$$\lim_{t \to 0} Q(t) \to t. \tag{75}$$

It follows from (74) that

$$J_R'(\delta') = \lim_{t \to \infty} Q(t) t^{\delta'-1} + \int_0^1 (1-\delta') Q(t) t^{\delta'-2} \, \mathrm{d}t + \int_0^1 (1-\delta') Q(1/t) t^{-\delta'} \, \mathrm{d}t \tag{76}$$

for $\delta' > 0$. One knows that the integral

$$\int_0^{\xi} \frac{\sin(x/2)}{x^{\delta'+1}} \, \mathrm{d}x \tag{77}$$

is convergent for $0 < \delta' < 1$. Because of the relation (75), the integral

$$\int_0^1 (1-\delta') Q(t) t^{\delta'-2} \, \mathrm{d}t \tag{78}$$

is always convergent for $\delta' > 0$. Now we can see that for $0 < \delta' < 1$, if

$$I_Q(\delta') = \int_0^1 Q(1/t) t^{-\delta'} \, \mathrm{d}t \tag{79}$$

converges (diverges), then $J_R(\delta')$ converges (diverges) and vice versa. We then prove the relation (67). Let us stress that here attention is only paid to the correspondence between the scaling δ and D_2, in the limit $t \to \infty$ and $l \to 0$. Keeping in mind the subtleties studied above in the scaling analysis of the autocorrelation function, a very careful treatment in the scaling analysis of the fractal dimension D_2 is also needed. In the following, we first study the periodic lattices to get some understanding about the influence of the subdominant term of $R(l)$ in evaluating the scaling D_2.

5.1. Periodic lattices

We still consider the 1D periodic chain, 2D square lattice and 3D cubic lattice. According to (66), $R(l)$ for those lattices is given by

$$R(l) = \frac{2}{\pi}\int_0^\infty J_0^{2D}(2\tau)\frac{\sin(l\tau/2)}{\tau}\,\mathrm{d}\tau. \tag{80}$$

Letting $x = t'/t$, from (10) we have

$$C(t) = \int_0^1 J_0^{2D}(2tx)\,\mathrm{d}x. \tag{81}$$

Now let $l\tau/2 = x$, from (80) one has

$$R(l) = \frac{2}{\pi}\int_0^1 J_0^{2D}\left(\frac{4}{l}x\right)\mathrm{d}x + I_B + I_C \tag{82}$$

with

$$I_B = \frac{2}{\pi}\int_0^1 J_0^{2D}\left(\frac{4}{l}x\right)\frac{\sin x - x}{x}\,\mathrm{d}x \tag{83}$$

$$I_C = \frac{2}{\pi}\int_1^\infty J_0^{2D}\left(\frac{4}{l}x\right)\frac{\sin x}{x}\,\mathrm{d}x \tag{84}$$

Since

$$x - \sin x \leqslant \left(1 - \frac{2}{\pi}\right)x \qquad 0 \leqslant x \leqslant \frac{\pi}{2} \tag{85}$$

we have

$$|I_B| < \left(1 - \frac{2}{\pi}\right)\frac{2}{\pi}\int_0^1 J_0^{2D}\left(\frac{4}{l}x\right)\mathrm{d}x. \tag{86}$$

Using the property (21) of the Bessel function, it is easy to find

$$I_C \sim l^D. \tag{87}$$

So we find that $R(l)$ (when $l \to 0$) has a similar behaviour to $C(t)$ (when $t \to \infty$), for both their dominant and subdominant parts. This is the reason why the previous calculation for D_2 of the spectral measure of the Fibonacci chain shows $D_2 = 0.84$ in the periodic limit [16]. Numerical calculations for the correlation dimensions D_2 of the spectra of 1D quasiperiodic systems such as the Harper model and the Fibonacci chain, have been carried out by Ketzmerick *et al* . The authors claimed that they found good agreement between the values for D_2 and δ. However, because of the way the scaling analysis was done, we have found it necessary to perform the numerical studies again, along the same lines as those discussed above.

Numerically, D_2 can be calculated by the box-counting technique. Dividing the energy range into boxes B_j of length l, $R(l)$ is then given by

$$R(l) = \sum_j \left[\int_{E\in B_j} \mathrm{d}\mu(E)\right]^2 \sim l^{D_2} \qquad l \to 0. \tag{88}$$

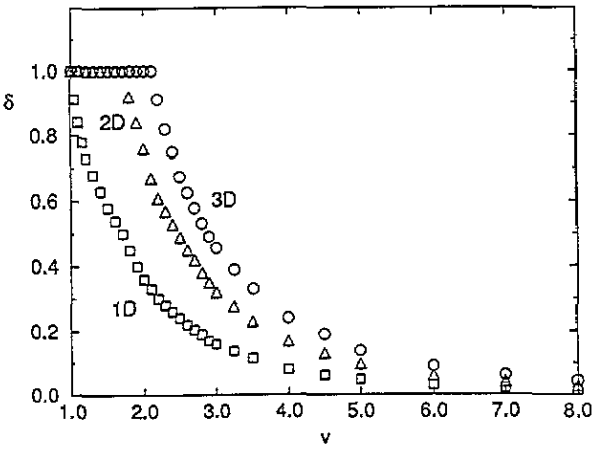

Figure 11. Exponent δ versus the modulation strength v for $C(t)(\sim t^{-\delta})$ in the 1D, 2D and 3D Fibonacci quasilattices (off-diagonal model).

5.2. Quasiperiodic systems

Figure 12 shows the scaling behaviour of the spectral probability $R(l)$ of the Harper model. To compare $R(l)$ with $C(t)$, we plot $\log R(l)$ and $\log C(t)$ together. From figure 12(a), one can see that

$$R(l) \sim C(1/l) \tag{89}$$

which gives $D_2 = \delta$ for $R(l) \sim l^{D_2}$ $(l \to 0)$ and $C(t) \sim t^{-\delta}$ $(t \to \infty)$. The agreement for $\lambda < 2$ can be more clearly seen in figure 12(b). The previous result [16] for $\lambda < 2$ suggested that $D_2 = 0.84$. Now we realize that this low estimated value comes from the logarithmic contribution which appears in $C(t)$, as discussed previously. In the case of $\lambda = 2$, $R(l)$ exhibits a periodic oscillation which has the same period as that of $C(t)$. This is why $C(t)$ displays periodic oscillatory behaviour. For the 1D Fibonacci chain, numerical results for various modulations confirm the existence of relation (89). As an example, the comparison between $R(l)$ and $C(t)$ for the Fibonacci chain (diagonal model) with $u = 0.1$ and $u = 0.5$ is illustrated in figure 13.

As stated above, the spectrum of the high-dimensional Fibonacci quasilattice can be obtained from that of the Fibonacci chain. From (38) and (40), it is easy to find [9] that the density of states of 2D and 3D Fibonacci quasilattices can be expressed as the convolution of the density of states of the Fibonacci chain

$$\text{2D} \qquad \rho(E) = \int \mathrm{d}E' \rho(E')\rho(E - E') \tag{90}$$

$$\text{3D} \qquad \rho(E) = \int\int \mathrm{d}E'\,\mathrm{d}E'' \rho(E')\rho(E'')\rho(E - E' - E''). \tag{91}$$

Moreover, according to the definition of the local density of states (LDOS), the LDOS at site (m, n) in 2D and (m, n, p) in 3D Fibonacci quasilattices are given by

$$\text{2D} \qquad \rho_{mn}(E) = \int \mathrm{d}E' \rho_m(E')\rho_n(E - E') \tag{92}$$

$$\text{3D} \qquad \rho_{mnp}(E) = \int\int \mathrm{d}E'\,\mathrm{d}E'' \rho_m(E')\rho_n(E'')\rho_p(E - E' - E''). \tag{93}$$

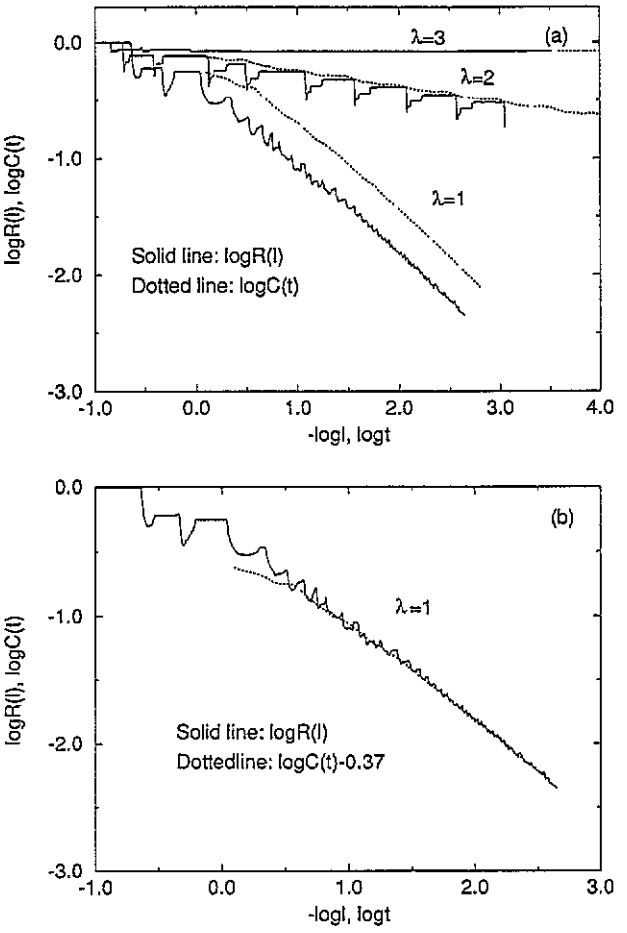

Figure 12. Probability $R(l)$ and autocorrelation function $C(t)$ for the Harper model: (a) $\lambda = 1, 2$ and 3; (b) $\lambda = 1$.

In our calculations, the LDOS of the Fibonacci chain is obtained by the RSRG techniques developed in [4]. Using (92) and (93), we can calculate the LDOS and $R(l)$ of the 2D and 3D Fibonacci lattices. Our results for $R(l)$ show that the relation (89) still holds. Instead of repeating the analysis to show this agreement, we now pay attention to the band structures. Figures 14 and 15 are the LDOS of 2D and 3D Fibonacci quasilattices (diagonal model) with various modulations. For the 2D system, one can see from figure 14 that the LDOS for $0 < u < 0.6$ is quite different from that for $u > 0.6$, which confirms the transition of the spectrum found by Ashraff et al [9], i.e., a transition from a spectrum with a finite number of gaps to one with an infinite number of gaps. For the 3D Fibonacci quasilattice, we find that a similar transition occurs near 0.9. This transition can be seen from the different behaviours of the LDOS illustrated in figure 15. This indicates that the critical values of the transition for the behaviour of $C(t)$ correspond to the critical values where the behaviour of the spectrum changes.

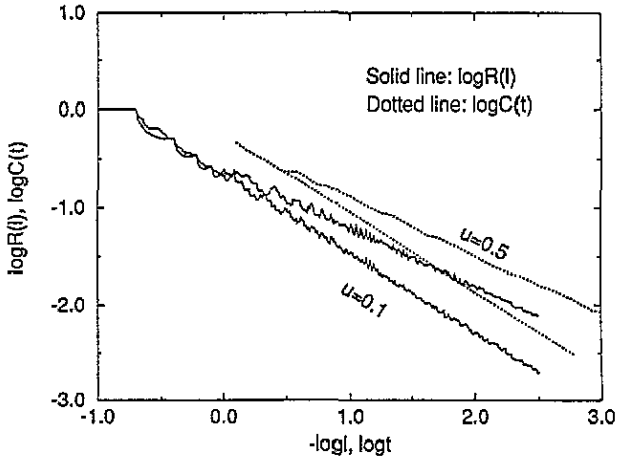

Figure 13. Probability $R(l)$ and autocorrelation function $C(t)$ for the Fibonacci chain (diagonal model) with $u = 0.1$ and $u = 0.5$.

6. Conclusion and discussion

We have studied the autocorrelation functions $C(t)$ of periodic lattices, the Harper model and the 1D, 2D and 3D Fibonacci quasilattices. It was found that, for all of these systems, $C(t)$ has a power-law decay $C(t) \sim t^{-\delta}$. We have emphasized that one should take care in the scaling analysis in order to get a correct picture of the decay of the autocorrelation function. The decays of $C(t)$, including their subdominant parts, have the following forms:

(1) Periodic lattices:

$$\text{1D} \qquad C(t) \sim (c_0 + c_1 \log t)t^{-1} \tag{94}$$

$$\text{2D} \qquad C(t) \sim (c_0 - c_1 t^{-1})t^{-1} \tag{95}$$

$$\text{3D} \qquad C(t) \sim (c_0 - c_1 t^{-2})t^{-1}. \tag{96}$$

The above relations give $\lim_{t\to\infty} \delta = 1$, which corresponds to the case of ballistic motion of the electron.

(2) Harper model:

$$\lambda < 2 \qquad C(t) \sim (c_0 + c_1 \log t)t^{-1} \tag{97}$$

$$\lambda > 2 \qquad C(t) \sim t^0 \tag{98}$$

$$\lambda = 2 \qquad C(t) \sim f(\log t)t^{-\delta} \qquad \delta = 0.13 \tag{99}$$

where $f(x)$ is a periodic function.

(3) 1D, 2D and 3D Fibonacci quasilattices
For diagonal models

$$\text{1D} \qquad C(t) \sim (c_0 + c_1 t^{\gamma})t^{-1} \qquad 0 < \gamma < 1 \tag{100}$$

$$\text{2D} \qquad C(t) \sim (c_0 - c_1 t^{-\gamma})t^{-1} \qquad 0 < \gamma < 1 \qquad (0 < u < u_c) \tag{101}$$

$$C(t) \sim (c_0 + c_1 t^{\gamma})t^{-1} \qquad 0 < \gamma < 1 \qquad (u > u_c) \tag{102}$$

$$\text{3D} \qquad C(t) \sim (c_0 - c_1 t^{-\gamma})t^{-1} \qquad 0 < \gamma < 2 \qquad (0 < u < u_c) \tag{103}$$

$$C(t) \sim (c_0 + c_1 t^{\gamma})t^{-1} \qquad 0 < \gamma < 1 \qquad (u > u_c) \tag{104}$$

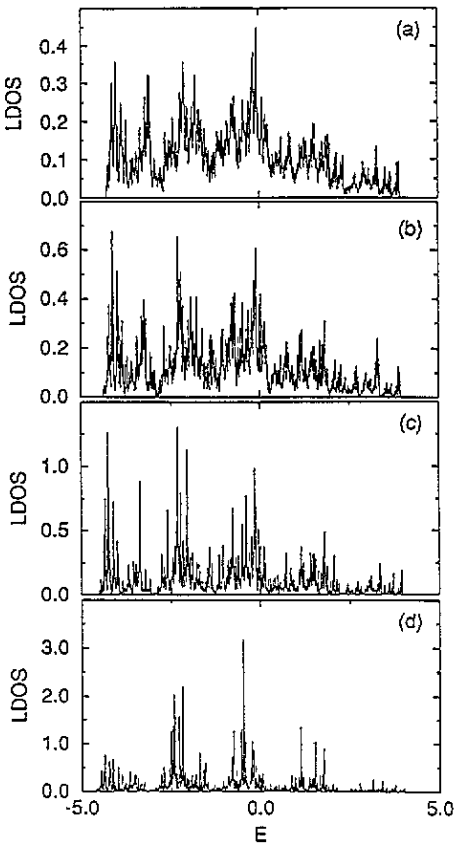

Figure 14. LDOS of the 2D Fibonacci quasilattice (diagonal model) with (a) $u = 0.4$, (b) $u = 0.5$, (c) $u = 0.6$, (d) $u = 0.7$.

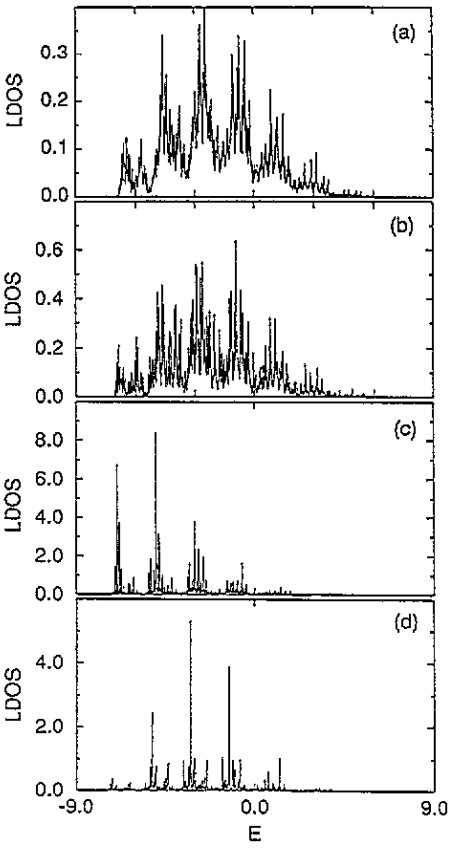

Figure 15. LDOS of the 3D Fibonacci quasilattice (diagonal model) with (a) $u = 0.7$, (b) $u = 0.8$, (c) $u = 0.9$, (d) $u = 1.0$.

where u is the modulation strength of the site energies and $u_c \approx 0.6$ and 0.9 for 2D and 3D Fibonacci quasilattices, respectively. For the off-diagonal model, we find similar properties. We have emphasized that, to correctly understand the nature of the dynamical behaviour of an electron, one should be very careful in the scaling analysis.

From (97), one can see that, for the Harper model with $\lambda < 2$, the decay of $C(t)$ has the same form as that of the 1D periodic lattice, i.e., $\lim_{t\to\infty} \delta = 1$. For the Harper model with $\lambda = 2$ and the Fibonacci chain, the decays of $C(t)$ have a scaling exponent $0 < \delta < 1$, showing that the motion of the electron is different from the ballistic motion found in periodic lattices. For the high-dimensional Fibonacci quasilattices, (101)–(104) strongly suggest that there exists a transition concerning the probability at the origin of the electron. Indeed, in the region $0 < u < u_c$, $\lim_{t\to\infty} C(t) \sim t^{-1}$ with the same exponent as that occuring in the case of ballistic motion in periodic lattices, while $C(t) \sim t^{-\delta}$ with $0 < \delta < 1$ when $u > u_c$.

We have also studied the relationship between the decays of the autocorrelation function $C(t)$ and the fractal dimension of the spectral measure. A proof is given, which shows that $R(l) \sim l^{\delta}$ $(l \to 0) \Longleftrightarrow C(t) \sim t^{-\delta}$ $(t \to \infty)$ for $0 < \delta < 1$, where $R(l)$ is the spectral probability of a singularly continuous or absolutely continuous measure with

bounded variation. The LDOS of 2D and 3D Fibonacci quasilattices indicate that the critical value u_c for the diagonal model or v_c for the off-diagonal model corresponds to that value where the spectrum changes behaviour from a band-like spectrum with finite number of gaps to another behaviour with an infinite number of gaps.

Acknowledgments

We thank J Bellissard, C Sire and A Ghazali for helpful discussions and comments.

References

[1] Harper P G 1955 *Proc. Phys. Soc. London* A **68** 874
Azbell M Ya 1964 *Soc. Phys.-JETP* **19** 634
Hofstadter D R 1976 *Phys. Rev.* B **14** 2239
Aubry S and Andre G 1980 *Ann. Israel Phys. Soc.* **3** 133
Tang C and Kohmoto M 1986 *Phys. Rev.* B **34** 2041
Bellissard J and Simon B 1982 *J. Func. Anal.* **48** 408
Socoloff D 1985 *Phys. Rep.* **126** 189
Simon B 1982 *Adv. Appl. Math.* **3** 463
[2] Kohmoto M, Kadanoff L P and Tang C 1983 *Phys. Rev. Lett.* **50** 1870
Ostlund S, Pandit R, Rand D, Schellnhuber H J and Siggia E D 1983 *Phys. Rev. Lett.* **50** 1873
Niu Q and Nori F 1986 *Phys. Rev. Lett.* **57** 2057
Luck J M 1986 *J. Physique* C **3** 205
Kohmoto M, Sutherland B and Tang C 1987 *Phys. Rev.* B **35** 1020
Sire C and Mosseri R 1989 *J. Physique* **50** 3447
Bellissard J, Iochum B, Scoppola E and Testard D 1989 *Commun. Math. Phys.* **125** 527
Süto A 1987 *Commun. Math. Phys.* **111** 409
[3] Sire C 1994 1991 *Lectures on Quasicrystals* ed F Hippert and D Gratials (Paris: Les Editions de Physique les Ulis) and references therein
Fujiwara T and Tsunetsugu K 1991 *Quasicrystals: The State of the Art* ed D P DiVincenzo and Steinhardt (Singapore: World Scientific) and references therein
[4] Zhong J X, You J Q, Yan J R and Yan X H *Phys. Rev.* B **43** 13778
Zhong J X, Yan J R, Yan X H and You J Q 1991 *J. Phys.: Condensed Matter* **3** 5685
[5] Zhong J X, Yan J R, You J Q, Yan X H and Mei Y P 1993 *Z. Phys.* B **91** 127
Zhong J X, Xie T, You J Q and Yan J R 1992 *Z. Phys.* **87** 223
[6] Zhong J X, Bellissard J and Mosseri R 1995 *J. Phys.: Condensed Matter* at press
[7] Sire C 1989 *Europhys. Lett.* **10** 483
[8] Ueda K and Tsunetsugu H 1987 *Phys. Rev. Lett.* **58** 1272
[9] Ashraff J A, Luck J M and Stinchcombe R B 1990 *Phys. Rev.* B **41** 4314
[10] Mayou D 1994 1983 *Lectures on Quasicrystals* ed F Hippert and D Gratials (Paris: Les Editions de Physique les Ulis), and references therein
[11] Casati G and Guarneri I *Phys. Rev. Lett.* **50** 640
[12] Bellissard J 1985 1987 *Trends and developments in the eighties* ed S Albeverio and P Blanchard (Singapore: World Scientific)
[13] Abe S and Hiramoto H *Phys. Rev.* A **36** 5349
Hiramoto H and Abe S 1988 *J. Phys. Soc. Japan* **57** 230 1365
[14] Guarneri I 1989 1991 *Europhys. Lett.* **10** 95; 1993 *Europhys. Lett.* **21** 729
[15] Geisel T, Ketzmerick R and Petschel G *Phys. Rev. Lett.* **66** 1651
[16] Ketzmerick R, Petschel G and Geisel T 1992 *Phys. Rev. Lett.* **69** 695
[17] Evangelou S N and Katsanos D E 1993 *J. Phys. A: Math. Gen.* **26** L1243
Katsanos D E, Evangelou S N and Xiong S J 1995 *Phys. Rev.* B **51** 895
[18] Wilkinson M and Austin E J 1994 *Phys. Rev.* B **50** 1420
[19] Passaro B, Sire C and Benza V G 1992 *Phys. Rev.* B **46** 13751
[20] Halsey T C, Jensen M H, Kadanoff L P, Procaccia I, and Shraiman B I 1986 *Phys. Rev.* A **33** 1141 and references therein